Thermolysis of the Osmium−Antimony Clusters Os₃(CO)₁₁(SbMe₂Ar): Higher Nuclearity Clusters and Arrested Ortho Metalation

Kiat Hwa Chan, Weng Kee Leong,* and Kar Hang Garvin Mak

Department of Chemistry, National University of Singapore, Kent Ridge, Singapore 119260

Thermolysis of the clusters $Os_3(CO)_{11}(SbMe_2Ar)$ (**1**, where Ar = Ph (**b**), *o*-tolyl (**c**), *p*-tolyl (**d**)), in refluxing octane gave the clusters $Os_3(\mu\text{-}SbMe_2)(\mu\text{-}H)(\mu_3,\eta^2\text{-}C_6H_3R)(CO)_9$ (**2,** where R = H (**b**), Me (**c**)), in good yields; both tolyl derivatives gave the same 4-substituted phenylene cluster. Among the minor products also isolated from the thermolysis of **1b** were the higher nuclearity clusters $Os_6(\mu_3\text{-}SbMe)\text{-}(\mu_3,\eta^2\text{-}C_6H_4)(CO)_{20}$ (**4**) and $Os_6(\mu_4\text{-}Sb)(\mu\text{-}SbMe_2)(\mu\text{-}H)(\mu_3,\eta^2\text{-}C_6H_4)_2(CH_3)(CO)_{16}$ (**5**), which contains an Os−CH₃ moiety. Thermolysis of the 3,5-xylyl analogue $Os_3(CO)_{11}\{SbMe_2(3,5\text{-}Me_2C_6H_3)\}$ (**1f**), on the other hand, gave the unusual species $Os_3(\mu\text{-}SbMe_2)(\mu_3,\eta^1{:}\eta^2{:}\eta^2\text{-}C_6H_3Me_2)(CO)_9$ (**6**), in which ortho metalation of the xylyl ring has apparently been arrested.

Introduction

Triosmium clusters containing a μ_3-phenylene ligand have been known from the very earliest work of Nyholm.[1] These clusters are commonly synthesized via thermolysis of clusters containing ligands with P−Ph,[1,2] As−Ph,[3] or S−Ph bonds.[4] The mode of coordination of the μ_3-phenylene group to the metal framework often depends on the other ligands that are on the cluster. The most common bonding mode is still the μ_3,η^2 mode, in which the phenylene acts as a four-electron donor.[5] These phenylene clusters have also been shown to be fluxional via ring flipping and hydride migration.[6] In addition, the mechanism for the formation of the phenylene clusters for the phosphine and arsine systems has been thoroughly investigated by Deeming.[2a,6] More recently, we have reported that thermolysis of the cluster $Os_3(CO)_{11}(SbPh_3)$ (**1a**) led initially to Sb−C cleavage to afford the cluster $Os_3(\mu\text{-}H)(\mu\text{-}SbPh_2)(\mu_3,\eta^2\text{-}$

$C_6H_4)(CO)_9$ (**2a**) in fairly good yield,[7] and this has allowed us to investigate the novel reactivity of this cluster.[8] As part of our investigations into the chemistry of this cluster, we had sought to understand its mode of formation and fluxional behavior in comparison with those of the phosphorus and arsenic analogues. We wish to report the results of our investigations here.

Results and Discussion

Deeming et al. have demonstrated the use of alkyl substituents on phosphine or arsine to control the thermolysis of the clusters $Os_3(CO)_{11}(EPh_2R)$ and $Os_3(CO)_{11}(EPhR_2)$, where E = P, As and R = alkyl.[6,9] The central idea was that the P−alkyl or As−alkyl bonds were less susceptible to thermolytic cleavage. We thus adopted the same idea in the hope of minimizing the formation of higher nuclearity clusters and thereby increase the yield of the initial benzyne product. Toward this goal, we have synthesized a number of stibine monosubstituted clusters $Os_3(CO)_{11}(SbR_3)$ (**1**, where R_3 = Me₂Ph (**b**), MePh₂ (**c**), Me₂[*o*-tolyl] (**d**), Me₂[*p*-tolyl] (**e**), SbMe₂[3,5-Me₂C₆H₃] (**f**), Me₃ (**g**)). The general reaction scheme employed is depicted in Scheme 1. The syntheses of the stibines were adapted from earlier published methods[10] and utilized Grignard reactions and a solid-state metathesis between SbCl₃ and SbAr₃.[11] The final step involved the use of the lightly stabilized cluster $Os_3(CO)_{11}\text{-}(NCCH_3)$.[12] The identities of **1b** and **1d** have also been confirmed by a single-crystal X-ray crystallographic study; the ORTEP plot showing the molecular structure of **1b** is given in Figure 1.

(1) (a) Bradford, C. W.; Nyholm, R. S. *J. Chem. Soc., Chem. Commun.* **1967**, 384. (b) Bradford, C. W.; Nyholm, R. S. *J. Chem. Soc., Dalton Trans.* **1973**, 529.

(2) (a) Brown, S. C.; Evans, J.; Smart, L. E. *J. Chem. Soc., Chem. Commun.* **1980**, 1021. (b) Deeming, A. J.; Kabir, S. E.; Powell, N. I.; Bates, P. A.; Hursthouse, M. B. *J. Chem, Soc., Dalton Trans.* **1987**, 1529. (c) Cullen, W. R.; Chacon, S. T.; Bruce, M. I.; Einstein, F. W. B.; Jones, R. H. *Organometallics* **1988**, *7*, 2273. (d) Deeming, A. J.; Marshall, J. E.; Nuel, D.; O'Brien, G.; Powell, N. I. *J. Organomet. Chem.* **1990**, *384*, 347. (e) Cullen, W. R.; Rettig, S. T.; Zhang, H. *Organometallics* **1991**, *10*, 2965. (f) Cullen, W. R.; Rettig, S. T.; Zhang, H. *Organometallics* **1992**, *11*, 928. (g) Cullen, W. R.; Rettig, S. T.; Zhang, H. *Organometallics* **1992**, *11*, 1000.

(3) (a) Arce, A. J.; Deeming, A. J. *J. Chem. Soc., Dalton Trans.* **1982**, 1155. (b) Johnson, B. F. G.; Lewis, J.; Massey, A. D.; Braga, D.; Grepioni, F. *J. Organomet. Chem.* **1983**, *251*, 261. (c) Jackson, P. A.; Johnson, B. F. G.; Lewis, J.; Massey, A. D.; Braga, D.; Gradella, C.; Grepioni, F. *J. Organomet. Chem.* **1990**, *391*, 225. (d) Cullen, W. R.; Rettig, S. T.; Zhang, H. *Organometallics* **1993**, *12*, 1964.

(4) Adams, R. D.; Katahira, D. A.; Yang, L. W. *Organometallics* **1982**, *1*, 235.

(5) Johnson, B. F. G.; Lewis, J.; Whitton, A. J.; Bott, S. J. *J. Organomet. Chem.* **1990**, *389*, 129.

(6) (a) Deeming, A. J.; Nyholm, R. S.; Underhill, M. *J. Chem. Soc., Chem. Commun.* **1972**, 224. (b) Deeming, A. J.; Kimber, R. E.; Underhill, M. *J. Chem., Soc., Dalton Trans.* **1973**, 2589. (c) Deeming, A. J.; Rothwell, I. P.; Hursthouse, M. B.; Backer-Dirks, J. D. J. *J. Chem, Soc., Dalton Trans.* **1981**, 1879. (d) Arce, A. J.; Deeming, A. J. *J. Chem. Soc., Dalton Trans.* **1982**, 1155. (e) Deeming, A. J.; Kabir, S. E.; Powell, N. I.; Bates, P. A.; Hursthouse, M. B. *J. Chem, Soc., Dalton Trans.* **1987**, 1529.

(7) Leong, W. K.; Chen, G. *Organometallics* **2001**, *20*, 2280.

(8) (a) Deng, M.; Leong, W. K. *Organometallics* **2002**, *21*, 1221. (b) Chen, G.; Deng, M.; Lee, C. K.; Leong, W. K. *Organometallics* **2002**, *21*, 1227.

(9) Cooksey, C. J.; Deeming, A. J.; Rothwell, I. P. *J. Chem. Soc., Dalton Trans.* **1981**, 1718.

(10) Pfeiffer, P.; Heller, I.; Pietsch, H. *Chem. Ber.* **1904**, *37*, 4620.
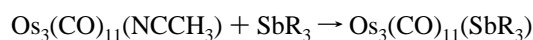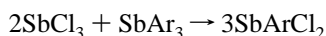
(11) (a) Nunn, M.; Sowerby, D. B.; Wesolek, D. M. *J. Organomet. Chem.* **1983**, *251*, C45. (b) Breunig, H. J.; Althaus, H.; Rösler, R.; Lork, E. *Z. Anorg. Allg. Chem.* **2000**, *626*, 1137.

(12) Nicholls, J. N.; Vargas, M. D. *Inorg. Synth.* **1989**, *28*, 232.
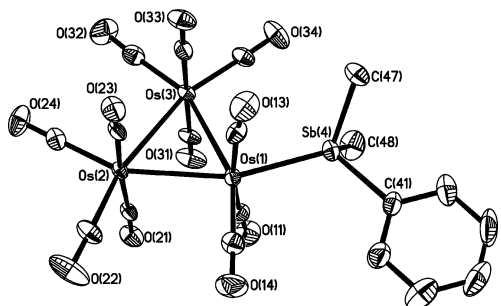
Figure 1. ORTEP diagram (organic hydrogens omitted, 50% probability thermal ellipsoids) for **1b**.

Scheme 1

$$SbCl_3 + 3ArMgBr \rightarrow SbAr_3$$

$$2SbCl_3 + SbAr_3 \rightarrow 3SbArCl_2$$

$$3SbArCl_2 + MeMgBr \rightarrow 3SbArMe_2$$

$$Os_3(CO)_{11}(NCCH_3) + SbR_3 \rightarrow Os_3(CO)_{11}(SbR_3)$$

Thermolysis of **1b** in refluxing octane indeed afforded the phenylene cluster $Os_3(\mu\text{-SbMe}_2)(\mu\text{-H})(\mu_3,\eta^2\text{-C}_6H_4)(CO)_9$ (**2b**) in a yield of 70%. Another cluster, $Os_3(\mu\text{-SbMe}_2)(\mu\text{-H})(\mu,\eta^2\text{-}C_6H_4)(CO)_{10}$ (**3**), and two higher nuclearity clusters, $Os_6(\mu_3\text{-}SbMe)(\mu_3,\eta^2\text{-C}_6H_4)(CO)_{20}$ (**4**) and $Os_6(\mu_4\text{-Sb})(\mu\text{-SbMe}_2)(\mu\text{-}H)(\mu_3,\eta^2\text{-C}_6H_4)_2(CH_3)(CO)_{16}$ (**5**), were also isolated together with $Os_3(CO)_{12}$ (**7**) (Scheme 2). All the new clusters, viz. **2b** and **3**−**5**, have been characterized completely, including by single-crystal X-ray crystallographic studies. The ORTEP plots showing their molecular structures are given in Figures 2−5, respectively.

Cluster **3** is a CO adduct of **2b**; it is structurally reminiscent of the group 15 and isonitrile adducts of **2a**.[13] Thermolysis of **3** gave **2b**, albeit in low yield, together with other as yet unidentified products, thus pointing to **3** as the precursor to **2b**. Cluster **4** is the methyl analogue of the previously reported $Os_6(\mu_3\text{-SbPh})(\mu_3,\eta^2\text{-C}_6H_4)(CO)_{20}$ (**4a**), obtained from the thermolysis of **1a**. Similarly, **5** is closely related to the previously reported cluster $Os_6(\mu_4\text{-Sb})(\mu\text{-SbPh}_2)(\mu\text{-H})(\mu_3,\eta^2\text{-C}_6H_4)_2(Ph)\text{-}(CO)_{16}$.[7] Cluster **2b** is stable up to about 125 °C, whereas the Sb−Ph bond in **2a** will cleave at about 90 °C. We therefore attempted the thermolysis of **1b** at a lower temperature (100
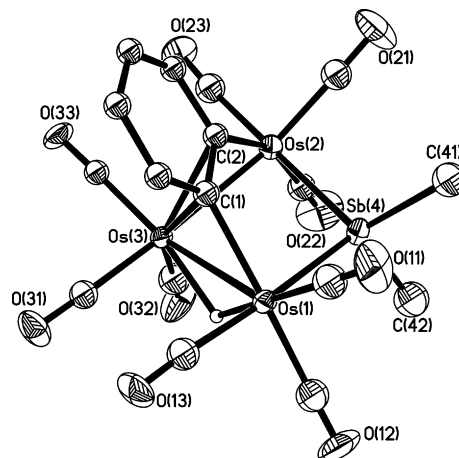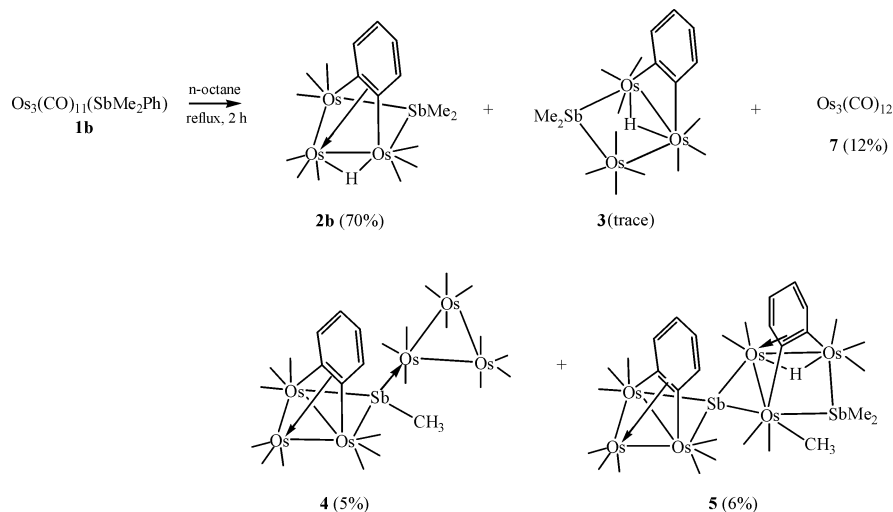

Figure 2. ORTEP diagram (organic hydrogens omitted, 50% probability thermal ellipsoids) for **2b**.

°C) for a longer period of time in the hope that the production of **4** and **5**, which required Sb−Me bond cleavage, would be decreased and thereby the yield of **2b** increased. Unfortunately, IR and ^{1}H NMR monitoring indicated that a steady state was reached, i.e., the signals due to **1b** and **2b** remained the same, after 1 h. That **7** was also formed suggested that it could represent the final stage of some eliminated species, and indeed when **1b** was thermolyzed with a small amount of **7** added, much of **1b** remained unreacted. The yields with respect to reacted **1b** were about 85% and 12% for **2b** and **7**, respectively; formation of **4** and **5** was not observed. This observation indicated that the formation of the clusters **2**−**5** probably required decarbonylation of **1b** as the rate-determining step.

The formation of **4** and **5** required Sb−CH$_3$ bond cleavage. This is in contrast to that observed for the phosphorus and arsenic systems; thermolysis of $Os_3(CO)_{11}(PR_3)$ (where R = Me, Et) afforded products from C−H bond activation,[14] while thermolysis of arsenic analogues such as $Os_3(CO)_{11}(AsMe_2Ph)$ afforded products resulting from metal−metal bond cleavage.[6b] This difference in their behavior is probably ascribable to the weaker Sb−C bond. As in the case of **1a**, the clusters **4** and **5** are probably derived from further reaction of **2b**. Thus, **4** is formally derived from **2b** via the loss of CH$_4$ and addition of an "$Os_3(CO)_{11}$" unit, while **5** is formally derived from the coupling of two units of **2b** via the loss of CH$_4$ and two carbonyl

Scheme 2[a]


2b (70%)

3 (trace)

7 (12%)

4 (5%)

5 (6%)

[a] Percent yields are with respect to reacted **1b**.
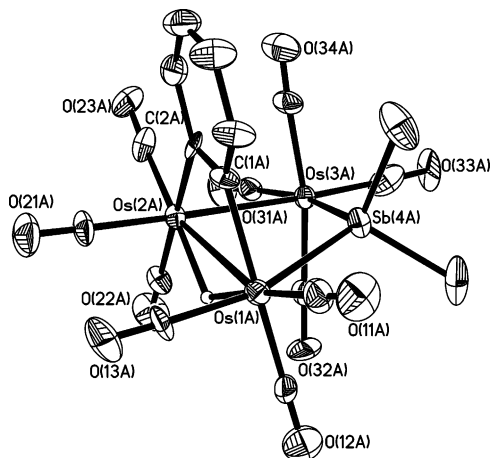
Figure 3. ORTEP diagram (organic hydrogens omitted, 50% probability thermal ellipsoids) for molecule A of **3**. Selected bond lengths (Å) and angles (deg) (molecules A, B): Os(1)−Os(2) = 3.1614(7), 3.1611(7); Os(2)−Os(3) = 2.9548(7), 2.9649(7); Os(1)−Sb(4) = 2.6430(10), 2.6820(12); Os(3)−Sb(4) = 2.6817(9), 2.6773(10); Os(1)−C(1) = 2.152(12), 2.116(13); Os(2)−C(2) = 2.142(12), 2.139(13); C(1)−C(2) = 1.384(18), 1.39(2); Os(2)−Os(1)−Sb(4) = 77.32(2), 78.10(3); Os(1)−Os(2)−Os(3) = 89.130(18), 89.39(2); Os(2)−Os(3)−Sb(4) = 80.52(2), 81.78(3); Os(1)−Sb(4)−Os(3) = 107.51(3), 107.11(4).
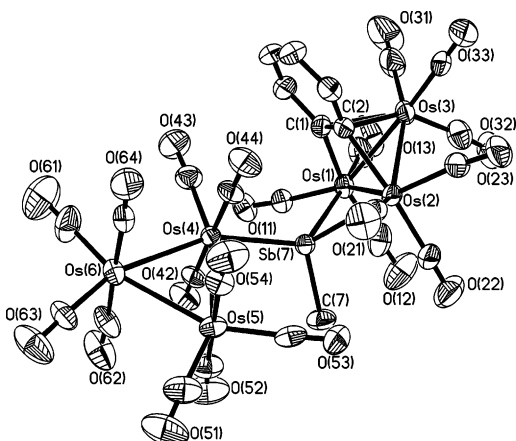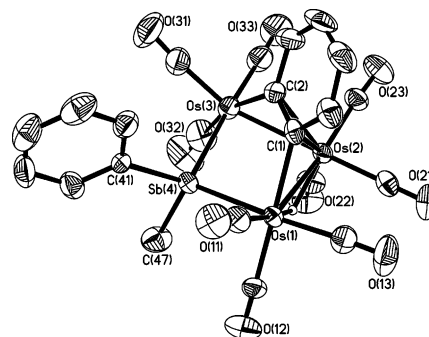

Figure 4. ORTEP diagram (organic hydrogens omitted, 50% probability thermal ellipsoids) for **4**.
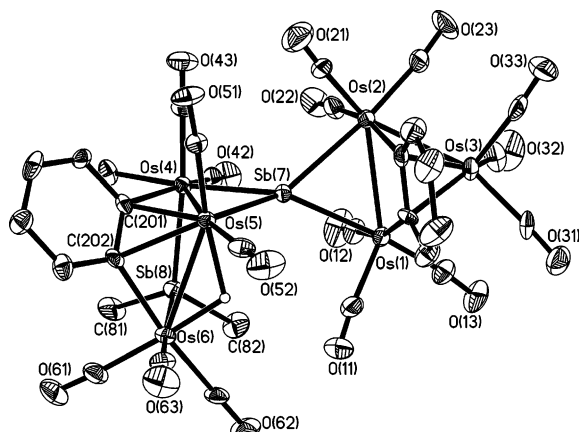
Figure 5. ORTEP diagram (organic hydrogens omitted, 50% probability thermal ellipsoids) for **5**.

ligands. Indeed, the thermolysis of **2b** in a Carius tube afforded **5** as the major product (29% isolated yield); refluxing decane was employed, as the reaction at refluxing octane temperature

Figure 6. ORTEP diagram (organic hydrogens omitted, 50% probability thermal ellipsoids) for **2c**.

was very slow. Analysis of the gas space above the solution by IR and GC indicated that CH_4 was indeed liberated; no C_2H_6 was detectable by IR, GC, or EI-MS.

The mean bond dissociation energies of the Sb−R bond in $SbPh_3$ and $SbMe_3$ (58.3 and 51.5 kcal mol^{-1}, respectively)[15] suggest that if the Sb−R bond cleavage was through a radical pathway, then the thermolysis of **1a** should have been less facile and that for **1g** the most facile. Instead, thermolysis of **1g** was difficult; only two products in extremely low yields were obtained, one of which has been characterized with the formulation "$Os_3SbMe_3(CO)_{10}$" (**8**), which is presumably related structurally to the previously reported cluster $Os_3(\mu\text{-}SbPh_2)(Ph)$-$(CO)_9(PPh_3)$.[8b] That no C_2H_6 was detected in the thermolysis also pointed to a nonradical pathway for the elimination of CH_4. This was also further corroborated by the failure to detect $TEMPO\text{-}CH_3$ when **2b** was thermolyzed in the presence of the radical trap TEMPO (2,2,6,6-tetramethyl-1-piperidinyloxy radical) in d_{20}-nonane.[16]

Working on the hypothesis that the formation of **4** therefore involved concerted CH_4 elimination, coupled with addition of an "$Os_3(CO)_{11}$" unit, which may possibly result from loss of $SbMe_2Ph$ from **1b** either simultaneously or sequentially (Scheme 3), we thermolyzed **1c** to obtain the pair of isomeric products **2c** and **2c′**. The ^1H NMR spectrum of the reaction mixture showed a 1:1 ratio of the two isomers. The isomers were not separable by TLC, but crystallization tended to give crystals of two slightly different colors (yellow and orange), which were separated by hand. Unfortunately, this did not turn out to be an absolutely foolproof means to distinguish between the two; at best, we managed to obtain samples that were either more of one or the other and hence allowed segregation of the ^1H resonances into two sets. Crystallographic analysis of one of the orange crystals (**2c**) established its molecular structure as that shown in Figure 6.

As mentioned above, there was ambiguity as to the assignments of the ^1H resonances to **2c** (that with the crystal structure established) and **2c′**. Nevertheless, we have made tentative assignments for the ^1H NMR resonances of **2a**, **2b**, **2c**, and **2c′**, particularly with regard to the last two, as shown in Figure 7. The $SbMe_2$ assignments are made in comparison with those for **6** (see below), for which the resonances were assigned on the

(13) (a) Chen, G.; Deng, M.; Lee, C. K.; Leong, W. K. *Organometallics* **2002**, *21*, 1227. (b) Chen, G.; Deng, M.; Lee, C. K. D.; Leong, W. K.; Tan, J.; Tay, C. T. *J. Organomet. Chem.*, in press.

(14) Deeming, A. J.; Underhill, M. *J. Chem. Soc., Dalton Trans.* **1973**, 2727.

(15) Skinner, H. A. *Adv. Organomet. Chem.* **1964**, *2*, 49.

(16) (a) Bowry, V.; Lusztyk, J.; Ingold, K. U. *Pure Appl. Chem.* **1990**, *62*, 213. (b) Skene, W. G.; Connolly, T. J.; Scaiano, J. C. *Int. J. Chem. Kinet.* **2000**, *32*, 238. (c) Bevington, J. C.; Warburton, J.; Hunt, B. J. *J. Macromol. Sci.* **2002**, *A39*, 1295.

Scheme 3
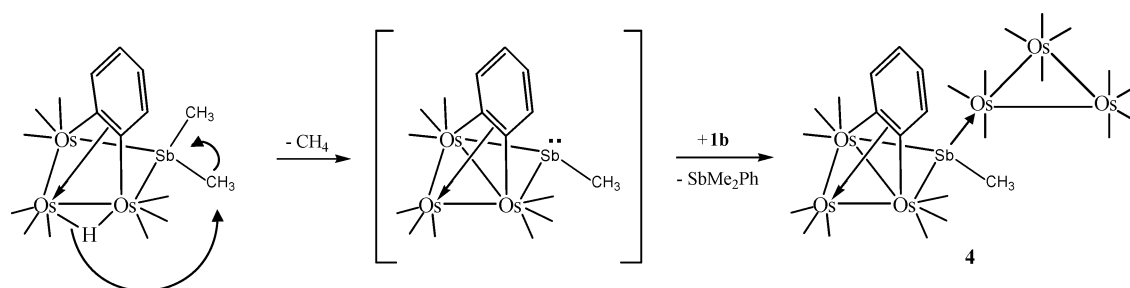
basis of a NOESY spectrum; the methyl group on the same side of the Os$_3$Sb plane as the phenylene resonated at higher field. The trend in the hydride resonances is clear and supports the structure assigned to **2c′**. We have also noticed that the resonances were temperature as well as solvent dependent. At room temperature, **2c** and **2c′** did not interconvert, even after standing in solution for several days. However, on mild heating, a solution of **2c** isomerized to afford a mixture containing equal amounts of **2c** and **2c′**. Such an isomerization was quite unexpected, and at this point we are unable to say what the mechanism may be.

The clusters **2c/2c′** also allowed us to make a direct comparison of the ease of elimination of a methyl vs a phenyl group from the antimony. Since the **2c−2c′** isomerization was also fast at elevated temperature, it was expected that **4** would be formed selectively over **4a**. An ESI-MS analysis of the reaction mixture when **2c/2c′** was thermolyzed with **1g** indeed showed that **4** was formed selectively over the phenyl analogue **4a**. This is thus consistent with the Sb−Ph bond being cleaved much more readily than the Sb−Me bond and also corroborated the pathway represented in Scheme 3.

Similarly, for the formation of **5**, we worked on the hypothesis that the same intermediate as that in Scheme 3 was involved. In this case, the nucleophilic attack was presumably on a second molecule of **2b**; we have already established such reactivity, for instance, in **2a**, which can undergo nucleophilic addition via a $\mu_3 \rightarrow \mu_2$ rearrangement of the phenylene followed by decarbonylation.[8b] Indeed, the position of substitution in **2a**, an axial site on the osmium across from the antimony, corresponds to where the intermediate "Os$_3$(μ_3-SbMe)(μ_3,η^2-C$_6$H$_4$)(CO)$_9$" will need to attack in order to form **5**. In this event, we observed

Table 1. Kinetic Parameters for the Aromatic Proton Exchanges in 2a−c

| compd	$\Delta H^{\ddagger}$ (kcal mol^{-1})	$\Delta S^{\ddagger}$ (cal mol^{-1} K^{-1})	$\Delta G^{\ddagger}_{300\ K}$ (kcal mol^{-1})
2a	14.0(9)	−3(3)	14.8(19)
2b	15.5(4)	2.1(12)	14.9(7)
2c	15.0(7)	0(3)	15.1(14)

that thermolysis of **2b** alone did afford **5**. The mode of transfer of the methyl group onto the second molecule of **2b** is uncertain.

As in the phosphorus and arsenic analogues, **2b** is fluxional. An EXSY spectrum taken at 300 K showed no exchange between the aromatic protons and the metal hydride. Simulation of the VT ^{1}H NMR behavior of the aromatic protons of the phenylene ring yielded a $\Delta G^{\ddagger}$(300 K) value of 14.9(7) kcal mol^{-1}, which is similar to that reported for the phosphorus analogue.[6a] It may thus be concluded that the fluxionality exhibited by **2b** is similar to that for the phosphorus analogue: viz., a combination of ring rotation and hydride migration. Similar analyses have also been carried out for **2a** and **2c**, and the kinetic parameters are summarized in Table 1. As an independent check, the $\Delta G^{\ddagger}$ values at the coalescence temperatures ($\sim$300−310 K) were also estimated, and the values for all three compounds were $\sim$14.1 kcal mol^{-1}.

Thermolysis of both the *o*- and *p*-tolyl analogues of **1b**, viz., Os$_3$(CO)$_{11}$\{SbMe$_2$(*o*-tol)\} (**1d**) and Os$_3$(CO)$_{11}$\{SbMe$_2$(*p*-tol)\} (**1e**), afforded the 4-substituted phenylene cluster Os$_3$(μ-SbMe$_2$)-(μ-H)(μ_3,η^2-C$_6$H$_3$-4-Me)(CO)$_9$ (**2d**) (Scheme 4). This behavior has also been observed with the arsenic analogue.[6d] Compound **2d** has been characterized completely, including by a single-crystal X-ray crystallographic study (Figure 8). The ^{1}H NMR
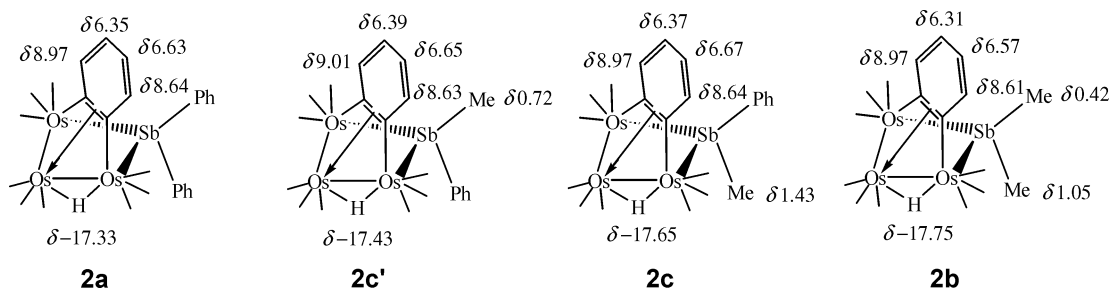
Figure 7. Tentative ^{1}H NMR (d_8-toluene, 238 K) assignments for **2a**, **2b**, **2c**, and **2c′**.

Scheme 4
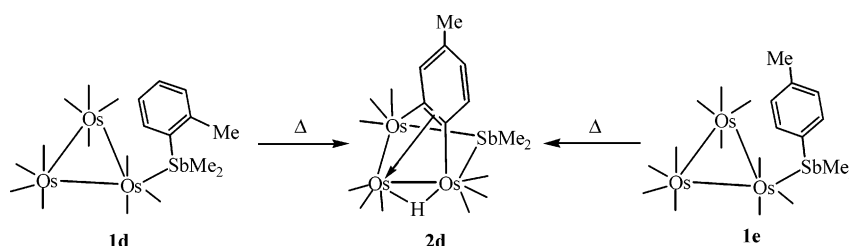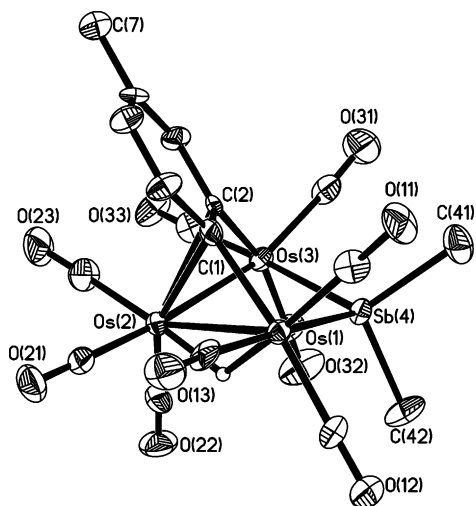
Figure 8. ORTEP diagram (organic hydrogens omitted, 50% probability thermal ellipsoids) for **2d**.

Figure 9. ORTEP diagram (organic hydrogens omitted, 50% probability thermal ellipsoids) for **6**.
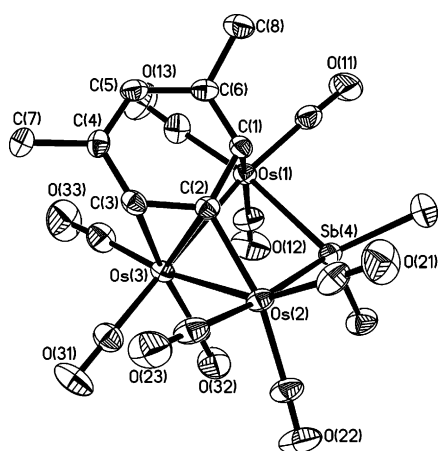
spectrum corresponds to the presence of two rapidly exchanging isomers. This has been tentatively ascribed to two diastereomeric forms which differ in the relative orientations of the hydride and the methyl group on the ring. At 215 K, the ratio of the diastereomers is 2.3:1.0, which is comparable to that reported for the arsenic analogue (2.1:1.0).[6d] That thermolyses of both **1d** and **1e** afforded **2d** meant that isomerization of the phenyl ring must have occurred at some point. However, as stated above, an EXSY experiment on **2b** showed that there was no aromatic proton−hydride exchange; a similar EXSY experiment on **2a** (90 °C, d_8-toluene) also gave similar results. These thus suggested that isomerization of the phenyl ring after formation of the *o*-phenylene cluster was not likely.

In an attempt to force the formation of a 3-substituted phenylene cluster, and to gain an understanding of the isomerization process, the xylyl analogue $Os_3(CO)_{11}\{SbMe_2(3,5-Me_2C_6H_3)\}$ (**1f**) was thermolyzed. The result was an unexpected xylyl-capping cluster, $Os_3(\mu\text{-}SbMe_2)(\mu_3,\eta^1:\eta^2:\eta^2\text{-}C_6H_3Me_2)$-$(CO)_9$ (**6**). The molecular structure of **6** has been confirmed by a single-crystal X-ray crystallographic study (Figure 9), and the ^1H resonances have been assigned with the aid of NOE correlations (Figure 10); NOESY cross-peaks were observed between the aromatic resonance at δ_H 6.46 and the methyl resonances at δ_H 2.89 and 2.11 ppm, between the aromatic resonance at δ_H 6.24 and the methyl resonances at δ_H 2.89 and 1.43 ppm, and between the resonances at δ_H 4.30 and 2.11 ppm.
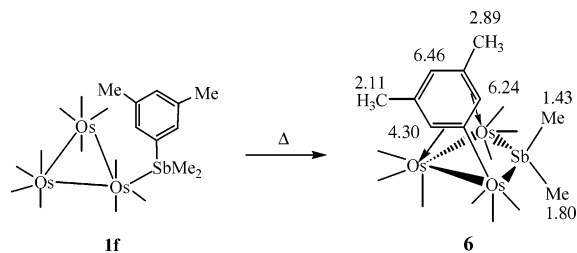
Figure 10. Thermolysis of **1f** to form **6** and the ^1H NMR assignments for **6**.

Scheme 5
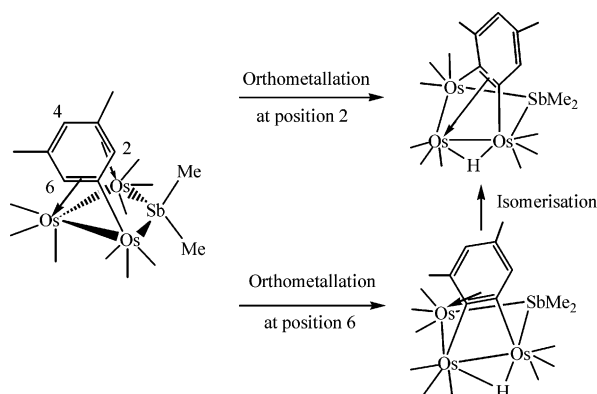
Cluster **6** represents the first example in which a phenyl ring adopts what appears to be an η^4 bonding mode to the triosmium cluster. A very similar structure has been proposed to be involved in the aromatic proton−hydride exchange in $Os_3(CO)_9$-$(\mu\text{-}H)_2(\mu_3,\eta^2\text{-}C_6H_4)$,[17] although a variable-temperature ^1H NMR study (d_8-toluene) on **6** showed it to be nonfluxional. Cluster **6** may also represent an intermediate in the formation of clusters **2**; ortho metalation at position 2 would yield the hypothetical *o*-phenylene cluster directly, whereas ortho metalation at position 6 would yield an isomer that can subsequently isomerize to the *o*-phenylene cluster itself (Scheme 5); the isomerization step has been demonstrated to occur in a PPh$_3$ derivative.[13a] The isolation of **6** may thus be a consequence of its inability to ortho metalate due to the sterically bulky Me groups at the two *meta* positions.

Structural Discussion. A common atomic numbering scheme and selected bond parameters for **1b** and both crystallographically independent molecules of **1d** are given in Table 2. It is interesting to note that the difference in bond parameters between the two crystallographically independent molecules of **1d** can be quite large; for example, the Os(2)−Os(3) and Os(1)−Sb(4) bond lengths differ by about 8σ and 7σ, respectively. This indicates that the effects of crystal-packing forces on structural parameters can be quite significant. As has been observed in numerous compounds of this type, the Os−Os bond cis to the stibine is lengthened relative to the others.[18] Likewise, the sums of Os−C and C−O bond distances[19] are noticeably longer for the axial than for the equatorial carbonyls (generally >3.06 Å for the former and <3.05 Å for the latter).

(17) Kneuper, H.-J.; Shapley, J. R. *Organometallics* **1987**, *6*, 2455.

(18) For example: (a) Biradha, K.; Hansen, V. M.; Leong, W. K.; Pomeroy, R. K.; Zaworotko, M. J. *J. Cluster Sci.* **2000**, *11*, 285. (b) Leong, W. K.; Liu, Y. *J. Organomet. Chem.* **1999**, *584*, 5267. (c) Bruce, M. I.; Liddell, M. J.; Hughes, C. A.; Skelton, B. W.; White, A. H. *J. Organomet. Chem.* **1988**, *347*, 157. (d) Bruce, M. I.; Liddell, M. J.; Hughes, C. A.; Patrick, J. M.; Skelton, B. W.; White, A. H. *J. Organomet. Chem.* **1988**, *347*, 181. (e) Hansen, V. M.; Ma, A. K.; Biradha, K.; Pomeroy, R. K.; Zaworotko, M. J. *Organometallics* **1998**, *17*, 5267.

(19) Leong, W. K.; Einstein, F. W. B.; Pomeroy, R. K. *J. Cluster Sci.* **1996**, *7*, 121.

Table 2. Common Atomic Numbering Scheme and Selected Bond Parameters for 1b and 1d
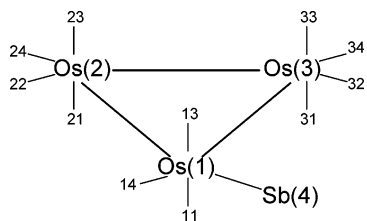
	1b	**1d** (molecule A)	**1d** (molecule B)
	Bond Lengths (Å)		
Os(1)−Os(2)	2.8463(3)	2.8494(8)	2.8500(8)
Os(2)−Os(3)	2.8898(3)	2.8902(8)	2.8835(8)
Os(1)−Os(3)	2.8981(3)	2.9062(7)	2.9065(8)
Os(1)−Sb(4)	2.5925(4)	2.5897(11)	2.5980(12)
	Bond Angle (deg)		
Os(2)−Os(1)−Os(3)	60.399(7)	60.274(19)	60.11(2)
Os(1)−Os(2)−Os(3)	60.687(7)	60.837(19)	60.91(2)
Os(2)−Os(3)−Os(1)	59.914(7)	58.889(18)	58.973(19)
Sb(4)−Os(1)−Os(3)	98.196(12)	98.64(3)	100.40(3)

A common atomic numbering scheme and selected bond parameters for **2a**−**d** are given in Table 3. The structure of **2a** has been reported previously;[7] that in this study is the dichloromethane solvate. As is to be expected, the longer Os−Os bond is that bridged by an hydride. This apparently also has further effects on the structures, such as the asymmetry in the Os−Sb and Os(2)−phenylene bond lengths. The Sb atom is tilted away from the Os_3 plane; the dihedral angle between the Os(1)Os(2)Os(3) and Os(1)Sb(4)Os(3) planes varies from about 22 to 28°. The phenylene ring is almost perpendicular to the Os_3 plane, the dihedral angle between the Os(1)Os(2)Os(3) plane and the phenylene ring being 70−75° but leaning slightly toward Os(2).

The crystal of **3** contained two crystallographically independent molecules; a common atomic numbering scheme and selected bond parameters are given in Table 4. Cluster **3** is of interest, as it may be regarded as the parent carbonyl (or more precisely, the dimethylantimony analogue of it) of the many derivatives which we have reported,[8b,13b] all of which contained an unusually long Os−Os bond. The derivatives which have been structurally characterized corresponded to substitution at CO(13) (PPh$_3$ and AsPh$_3$), CO(21) (PPh$_3$, P(p-tolyl)$_3$, and ^{t}BuNC), and CO(32) (^{t}BuNC). As in those derivatives, the Os−Os bond bridged by the μ,η^2-phenylene is very long, although within this class of compounds that for **3** (3.1614(7) and 3.1611(7) Å, respectively, for the two molecules) is the shortest. This thus corroborated our contention that the elongation of this Os−Os bond is partly due to steric repulsion of any ligand substituted at Os(1) or Os(2) with carbonyls on the adjacent osmium. Similarly, the Os(2)−Os(3) bond length in **3** is also shorter than any among the substituted derivatives, in agreement with ligand effects in the latter. Finally, it is noted that, as for **1d**, chemically equivalent bond parameters can differ very significantly. For instance, even the Os(2)−Os(3) bond lengths differ by 14σ between the two molecules.

As mentioned above, the diphenylantimony analogue of **4**, viz., Os$_6$(μ_3-SbPh)(μ_3,η^2-C$_6$H$_4$)(CO)$_{20}$ (**4a**), has been reported by us earlier,[7] while **5** is closely related to the previously reported cluster Os$_6$(μ_4-Sb)(μ-SbPh$_2$)(μ-H)(μ_3,η^2-C$_6$H$_4$)$_2$(Ph)-(CO)$_{16}$ (**5a**). Cluster **5** differs from **5a** in that a dimethylantimony moiety in **5** replaces the diphenylantimony moiety in **5a**, and also there is a methyl group on Os(4) in the former instead of a phenyl group on Os(3) in the latter. Cluster **5** is a very rare example of an osmium cluster containing an alkyl ligand, as

Table 3. Common Atomic Numbering Scheme and Selected Bond Parameters for 2a−d
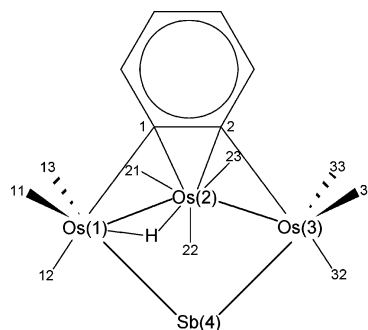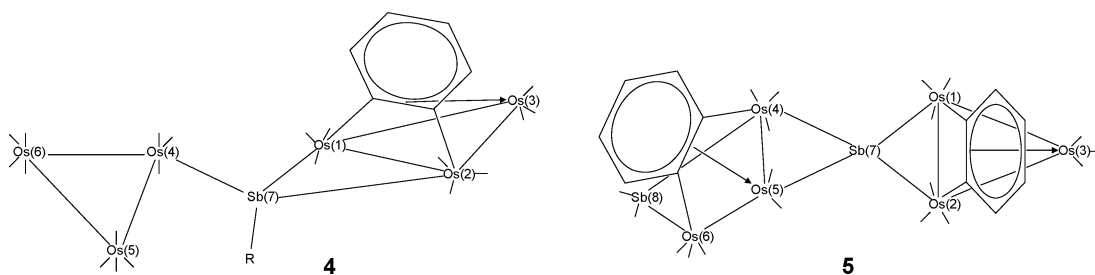

	2a	**2b**	**2c**	**2d**
	Bond Lengths (Å)			
Os(1)−Os(2)	2.9493(8)	2.9631(9)	2.9563(4)	2.9597(7)
Os(2)−Os(3)	2.8517(8)	2.8449(9)	2.8356(4)	2.8547(7)
Os(1)−Sb(4)	2.6571(10)	2.6324(13)	2.6437(5)	2.6341(9)
Os(3)−Sb(4)	2.6403(10)	2.6272(13)	2.6365(5)	2.6257(9)
Os(1)−C(1)	2.172(15)	2.174(16)	2.177(7)	2.175(12)
Os(3)−C(2)	2.217(13)	2.140(16)	2.167(7)	2.150(13)
Os(2)−C(1)	2.325(15)	2.309(16)	2.352(6)	2.321(13)
Os(2)−C(2)	2.388(14)	2.357(16)	2.369(6)	2.379(11)
C(1)−C(2)	1.431(19)	1.45(2)	1.444(9)	1.489(18)
	Bond Angles (deg)			
Os(2)−Os(1)−Sb(4)	83.69(3)	82.78(3)	82.895(13)	81.76(2)
Os(1)−Os(2)−Os(3)	87.79(2)	87.57(2)	87.853(10)	87.721(19)
Os(2)−Os(3)−Sb(4)	85.94(3)	85.22(3)	85.410(13)	83.95(2)
Os(1)−Sb(4)−Os(3)	98.82(3)	99.68(4)	99.128(16)	100.01(3)
	Dihedral Angles (deg)			
Os(1)Os(2)Os(3)/ Os(1)Sb(4)Os(3)	21.5	24.3	24.2	28.7
Os(1)Os(2)Os(3)/ phenylene	72.3	70.2	74.8	70.7

these tend to undergo C−H activation.[20] A common atomic numbering scheme and selected bond parameters for all four of these clusters are given in Table 4.

Structurally, the clusters **4** and **5** can be regarded as being derived from an Os$_3$(μ_3,η^2-C$_6$H$_4$)(CO)$_9$(u-SbR$_2$) fragment; in the case of **4** and **4a**, one R group on the antimony has been replaced by an Os$_3$(CO)$_{11}$ unit, while in **5** and **5a**, both R groups have been replaced by another Os$_3$(μ_3,η^2-C$_6$H$_4$)(CO)$_9$(u-SbR$_2$) fragment, together with further substitution of a carbonyl by a methyl or phenyl. Clusters **4** and **4a** are structurally very similar. It appears that the bond lengths involving the heavy atoms (but not the light atoms, such as in the phenylene ring) are all shorter in **4** than in **4a**, although there is no obvious reason why this should be so. In all four clusters, within the phenylene-bridged Os$_3$ units, the Os(1)−Os(2) bond is the longest. In the case of **5** and **5a**, this bond length is quite similar but the other Os−Os bonds in that fragment are longer in **5a**, presumably due to the greater σ donation from the phenyl on Os(3).

A schematic diagram of **6**, together with selected bond parameters, is given in Figure 11. The interpretation of the bonding between the xylyl ring and the cluster is interesting. The Os(1)···Os(2) distance of ∼4.044 Å is clearly nonbonding, and both the structural refinement and ^{1}H NMR spectrum indicate the absence of any metal hydride. The valence electron count therefore requires the xylyl to act as a five-electron donor. We have therefore chosen this to result from a C(2)−Os(2) σ bond and donation of the C(2)−C(3) and C(1)−C(6) π electrons.

(20) (a) Cree-Uchiyama, M.; Shapley, J. R.; St. George, G. M. *J. Am. Chem. Soc.* **1986**, *108*, 1316. (b) Boyar, E.; Deeming, A. J.; Arce, A. J.; De Sanctis, Y. *J. Organomet. Chem.* **1984**, *276*, C45. (c) Keister, J. B.; Shapley, J. R. *J. Am. Chem. Soc.* **1976**, *98*, 1056.

Table 4. Common Atomic Numbering Scheme and Selected Bond Parameters for 4 and 5 and Their Analogues

	4	4a[a]	5	5a
R	Me	Ph	Me on Os(4)	Ph on Os(3)
		Bond Lengths (Å)		
Os(1)−Os(2)	2.9019(5)	2.9095(11), 2.9101(11)	2.9057(6)	2.8943(9)
Os(2)−Os(3)	2.7831(5)	2.7939(12), 2.8024(10)	2.7653(5)	2.8188(9)
Os(3)−Os(1)	2.7524(6)	2.7739(10), 2.7659(12)	2.7696(5)	2.8466(9)
Os(4)−Os(5)	2.9056(5)	2.9133(12), 2.9174(10)	2.9333(5)	2.9422(8)
Os(5)−Os(6)	2.8746(5)	2.8910(12), 2.8824(11)	2.9481(5)	2.9113(9)
Os(6)−Os(4)	2.8470(5)	2.8704(11), 2.8794(10)		
Os(1)−Sb(7)	2.7171(7)	2.7240(16), 2.7263(13)	2.6966(7)	2.6306(11)
Os(2)−Sb(7)	2.6902(7)	2.7170(14), 2.7201(15)	2.7066(7)	2.6474(12)
Os(4)−Sb(7)	2.6032(7)	2.6327(15), 2.6344(14)	2.6589(7)	2.7664(11)
Os(5)−Sb(7)			2.5515(7)	2.5376(11)
Os(4)−Sb(8)			2.6524(7)	2.6621(12)
Os(6)−Sb(8)			2.6553(8)	2.6310(11)
Sb(7)−R	2.156(9)	2.180(18)		
Os−R			2.205(9)	2.133(17)
		Bond Angles (deg)		
Os(2)−Os(1)−Os(3)	58.900(13)	58.83(3), 59.11(3)	58.260(13)	58.81(2)
Os(1)−Os(2)−Os(3)	57.870(13)	58.16(3), 57.88(3)	58.406(13)	59.75(2)
Os(1)−Os(3)−Os(2)	63.231(13)	63.01(3), 63.01(3)	63.333(14)	61.44(2)
Os(5)−Os(4)−Os(6)	59.950(13)	59.98(3), 59.63(3)	-	-
Os(4)−Os(5)−Os(6)	59.014(12)	59.28(3), 59.53(2)	87.408(14)	88.52(2)
Os(4)−Os(6)−Os(5)	61.036(13)	60.75(3), 60.84(3)		
Os(5)−Os(4)−Sb(7)	96.363(17)	98.56(4), 97.64(4)	54.022(16)	52.68(2)

[a] Contains two crystallographically independent molecules.
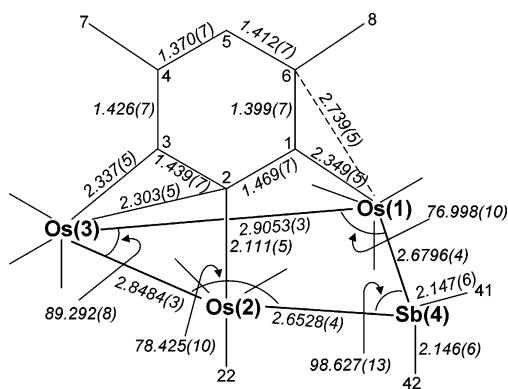
Figure 11. Schematic diagram of **6**, with selected bond lengths (Å) and angles (deg).

The Os(2)−C(2) bond length of 2.111(5) Å is comparable to, for instance, the Os−phenyl bond length in **5a**, and so to regard the xylyl ring as being σ bonded to Os(2) appears reasonable. This σ donation from the aromatic ring is also manifested in its effect on CO(22); the sum of the Os(2)−C(22) and C(22)−O(22) bond lengths is 3.07 Å,[19] significantly longer than for the other carbonyls, which are all below about 3.06 Å. The Os(3)−C lengths are fairly close to the ~2.30 Å observed for the π-bond donation to Os observed in, for example, all four of the clusters **4** and **5** above, although there is asymmetry here. This indicates that there is an equivalent donation of the π electrons along the C(2)−C(3) bond to Os(3). This is also corroborated by the C(2)−C(3) bond length, which is longer than that in a normal aromatic ring. Interestingly, there is an

alternation to the C−C bond lengths around the xylyl ring which suggests that the double bonds are fairly localized. The interpretation that there is an interaction of the C(1)−C(6) π bond with Os(1) is a bit more problematic. As the bond parameters indicate, this last interaction is at best a very weak one (the next closest Os···C(xylyl) distance is that of Os(1)···C(2) at 2.960(5) Å). This is also apparent from the ^{1}H resonances; δ_H for H(1) is 6.24 ppm, compared to 4.30 ppm for H(3); this is clearly indicative of the aromatic nature of the former and the more alkenic nature of the latter. It is therefore possible that **6** may have some degree of electron deficiency. This is consistent with the red color of **6**, as electron-precise triosmium clusters are usually yellow; if they are electron deficient, their colors shift to a darker shade.

Concluding Remarks

In this report, we have examined the thermolyses of a number of clusters of the formulas $Os_3(CO)_{11}(SbMe_2Ar)$, to control the product distribution. The fluxional behaviors of the clusters containing the *o*-phenylene moiety have been examined and their kinetic parameters determined. Higher nuclearity clusters have also been obtained, including one which contains a rare Os−alkyl bond. Studies directed at understanding the mechanistic pathways of these thermolytic reactions have also been carried out, and we have determined that the Sb−C bond cleavage probably does not proceed via a radical mechanism. An unusual cluster containing an η^4-bonded aromatic ring has also been obtained, which we believe is an intermediate that has been arrested in the process of ortho metalation.

Experimental Section

General Procedures. All reactions and manipulations were carried out under nitrogen using standard Schlenk techniques.[21] Solvents were purified, dried, distilled, and stored under nitrogen prior to use. The products were generally separated by column chromatography on silica gel 60 (230−430 mesh ASTM) or by thin-layer chromatography (TLC), using plates coated with silica gel 60 F254 of 0.25 mm or 0.5 mm thickness and extracted with hexane or dichloromethane. Solution IR spectra were recorded in hexane unless otherwise indicated. Gaseous state IR spectra were acquired in a gas cell (15 cm path length) with KBr windows. Routine NMR spectra were recorded as $CDCl_3$ solutions, unless otherwise stated, on a Bruker ACF-300 FT NMR spectrometer. [1]H chemical shifts reported are referenced against the residual proton signals of the solvents. Selective decoupling experiments, spin saturation transfer, variable-temperature, and 2D spectra (EXSY, NOESY) were acquired on a Bruker Avance DRX500 or Bruker AMX500 machine. NMR simulations were carried out with the gNMR program.[22] Mass spectra were obtained on a Finnigan MAT95XL-T spectrometer in an *m*-nitrobenzyl alcohol matrix. GC analyses were carried out on a Hewlett-Packard 5890 Series 2 PLUS gas chromatograph with a flame ionization detector and a Chrompack CP-Silica fused silica column (30 m length × 0.32 mm i.d.). Microanalyses were carried out by the microanalytical laboratory at the National University of Singapore. The cluster $Os_3(CO)_{11}$-$(NCCH_3)$ was prepared according to the literature method.[12] All other reagents were from commercial sources and used as supplied.

Preparation of SbMePh₂. To a suspension of CH_3I (0.51 mL, 8.24 mmol) and Mg turnings (0.241 g, 9.897 mmol) in tetrahydrofuran (30 mL) was added dropwise a solution of $SbPh_2Cl$ (2.276 g, 7.311 mmol) in tetrahydrofuran (20 mL). The reaction mixture was stirred at room temperature for 12 h, whereupon a dirty green suspension was obtained. The solvent was removed in vacuo, and the liquid residue was extracted with 80 mL of hexane. The colorless supernatant was transferred via cannula into a Schlenk flask and stored under nitrogen.

Spectroscopic data are as follows. ^{1}H NMR: δ 7.56−7.47 (m, 4H), 7.36−7.33 (m, 6H), 0.96 (s, 3H). EIMS: *m/z* (% relative intensity, ion) 291 (71, M), 275 (80, M − Me), 211 (14, M − Ph), 198 (62, M − Ph − Me), 136 (5, M − 2Ph). HR-EI MS: *m/z* [M]⁺ calcd for $C_{13}H_{13}{}^{121}Sb$, 290.0055; $C_{13}H_{13}{}^{123}Sb$, 292.0059; found 290.0057, 292.0060 (respectively).

Preparation of $Os_3(CO)_{11}(SbMe_2Ph)$ (1b). To $Os_3(CO)_{11}(CH_3$-CN) (190 mg, 0.206 mmol) was added $SbMe_2Ph$ (50 mg, 0.220 mmol) in dichloromethane (40 mL). The reaction mixture was stirred at 60 °C for 6 h. Silica gel was then added and the solvent was removed in vacuo, followed by column chromatographic separation, to give $Os_3(CO)_{12}$ (6.4 mg, 3.4%, identified by IR spectroscopy), yellow crystalline **1b** (182.6 mg, 80.1%), and yellow oily $Os_3(CO)_{10}(SbMe_2Ph)_2$ (28.0 mg, 10.4%, identified by comparing its IR spectrum with those of analogous bis-substituted triosmium clusters).

Data for **1b** are as follows. IR: $\nu(CO)$ 2108 (w), 2056 (s), 2032 (m), 2021 (vs), 2004 (vw), 1991 (w), 1971 (w), 1955 (vw) cm⁻¹. ^{1}H NMR: δ 7.58−7.47 (m, 5H, Ph), 1.63 (s, 6H, Me) ppm. Anal. Calcd for $C_{19}H_{11}O_{11}Os_3Sb$: C, 20.60; H, 1.00. Found: C, 20.83; H, 0.97.

Details of the preparation and spectroscopic characterization of **1c−g** and their organostibine precursors are given in the Supporting Information.

Thermolysis of 1b in Refluxing *n*-Octane. Cluster **1b** (180.0 mg, 0.162 mmol) was thermolyzed in refluxing *n*-octane (150 mL)

(21) Shriver, D. F.; Drzedzon, M. A. *The Manipulation of Air-Sensitive Compounds*, 2nd ed.; Wiley: New York, 1986.
(22) Budzelaar, P. H. M. gNMR; Adept Scientific plc, Letchworth, U.K., 1999.

under constant nitrogen bubbling until the color of the solution turned from yellow to orange (∼1.5 h). The solvent was then removed in vacuo, and the residue was redissolved in the minimal volume of dichloromethane for separation by TLC on silica (eluant: hexane).

Band 1 (R_f = 0.67): $Os_3(CO)_{12}$ (**7**). Yield: 12.0 mg, 8.2%. Identified by IR spectroscopy.

Band 2 (R_f = 0.45): yellow crystals of $Os_3(CO)_9(\mu$-H)$(\mu_3,\eta^2$-$C_6H_4)(\mu$-SbMe_2)$ (**2b**). Yield: 80.1 mg, 47.2%. IR: $\nu(CO)$ 2089 (w), 2068 (vs), 2040 (vs), 2009 (vs), 2003 (m, sh), 1988 (w), 1976 (w), 1968 (w) cm⁻¹. ^{1}H NMR (233 K): δ 9.15 (d, 1H, ${}^3J_{HH}$ = 8.25 Hz, aromatic), 6.76 (dd, 1H, aromatic), 7.00 (dd, 1H, aromatic), 8.67 (d, 1H, aromatic), 1.57 (s, 3H, Me), 1.11 (s, 3H, Me), −17.71 (s, 1H, OsHOs) ppm. FAB-MS: *m/z* 1051.8 (calcd for [M⁺] 1051.6). Anal. Calcd for $C_{17}H_{11}O_9Os_3Sb\cdot{}^1/_4C_6H_{14}$: C, 20.70; H, 1.36. Found: C, 20.52; H, 1.17. ^{1}H NMR confirms the presence of hexane in the sample.

Band 3 (R_f = 0.43): yellow. Unidentified mixture. Yield: <2 mg.

Band 4 (R_f = 0.42): yellow crystalline solids of $Os_3(\mu$-SbMe_2)$-$(\mu$-H)$(\mu,\eta^2$-$C_6H_4)(CO)_{10}$ (**3**). Yield: <2 mg. IR: $\nu(CO)$ 2105 (w), 2083 (vs), 2064 (s), 2034 (m), 2024 (vs), 2015 (m), 2011 (s), 2002 (w), 1991 (w), 1989 (sh) cm⁻¹. ^{1}H NMR: δ 7.46 (d, 1H, ${}^2J_{HH}$ = 7.4 Hz, aromatic), 7.27 (d, 1H, ${}^2J_{HH}$ = 7.4 Hz, aromatic), 6.93 (dd, 1H, aromatic), 6.77 (dd, 1H, aromatic), 1.54 (s, 3H, Me), 0.61 (s, 3H, Me), −20.43 (s, 1H, OsHOs). Anal. Calcd for $C_{18}H_{11}O_{10}$-Os_3Sb: C, 20.02; H, 1.03. Found: C, 20.25; H, 0.96.

Band 5 (R_f = 0.40): unreacted **1b**. Yield: 59.1 mg. Identified by IR spectroscopy.

Band 6 (R_f = 0.20): red crystals of $Os_6(CO)_{20}(\mu_3,\eta^2$-$C_6H_4)(\mu_3$-SbMe) (**4**). Yield: 5.4 mg, 3.5%. IR: $\nu(CO)$ 2094 (m), 2065 (m, sh), 2058 (s), 2022 (vs) cm⁻¹. ^{1}H NMR (CD_2Cl_2) δ: 7.88 (dd, ${}^3J_{HH}$ = 6.60 Hz, ${}^4J_{HH}$ = 3.30 Hz, 1H, aromatic), 7.78 (dd, 1H, aromatic), 6.78 (dd, ${}^3J_{HH}$ = 6.60 Hz, ${}^4J_{HH}$ = 3.30 Hz, 2H, aromatic), 2.25 (s, 3H, Me) ppm. FAB-MS: *m/z* 1914.4 (calcd for [M⁺] 1914.3). Anal. Calcd for $C_{27}H_7O_{20}Os_6Sb\cdot{}^1/_4C_6H_{14}$: C, 17.68; H, 0.55. Found: C, 17.52; H, 0.58. ^{1}H NMR confirms the presence of hexane in the sample.

Band 7 (R_f = 0.15): dark red crystals of $Os_6(CO)_{16}(CH_3)(\mu$-H)-$(\mu_3,\eta^2$-$C_6H_4)_2(\mu_4$-Sb)$(\mu$-SbMe_2)$ (**5**). Yield: 6.6 mg, 4.0%. IR (CH_2Cl_2): $\nu(CO)$ 2099 (m), 2078 (m), 2067 (s), 2054 (vs), 2026 (vs), 2014 (vs), 2011 (vs, sh), 1962 (w) cm⁻¹. ^{1}H NMR (CD_2Cl_2): δ 9.06 (d, 1H, ${}^3J_{ab}$ = 7.44 Hz, H_a), 8.49 (d, 1H, ${}^3J_{cd}$ = 7.44 Hz, H_d), 7.93 (d, 1H, ${}^3J_{ef}$ = 9.06 Hz, H_e), 7.55 (dd, 1H, ${}^3J_{fg}$ = 9.06 Hz, H_f), 7.46 (dd, 1H, ${}^3J_{gh}$ = ${}^3J_{fg}$ = 9.06 Hz, H_g), 7.33 (d, 1H, H_h), 6.94 (dd, 1H, ${}^3J_{bc}$ = 7.44 Hz, H_c), 6.82 (dd, 1H, H_b), 1.27 (s, 3H, Me), 0.91 (s, 3H, Me), 0.81 (s, 3H, Me), −16.30 (s, 1H, OsHOs). Anal. Calcd for $C_{31}H_{18}O_{16}Os_6Sb_2\cdot2C_6H_{14}$: C, 23.44; H, 2.10. Found: C, 23.38; H, 1.89. The ^{1}H NMR spectrum of the sample confirms the presence of hexane.

Cluster **3** was obtained in a yield of 19.3 mg (8.0%) from a reaction in which a larger quantity (300 mg) of **1b** was used.

A similar thermolysis of **1b** (5.2 mg, 0.0047 mmol) at 100 °C was monitored by IR at 30 min intervals until no further change in the reaction spectrum was observed. Workup afforded unreacted **1b** (4.8 mg) and **2b** (0.3 mg, 6.1%).

Thermolysis of 1b in a Carius Tube. Cluster **1b** (6.3 mg, 0.0057 mmol) was placed in a Carius tube with distilled *n*-heptane (10 mL), degassed by three freeze−pump−thaw cycles, and then heated at 125 °C for 15 h. The color of the solution turned from yellow to brown. The solution was then cooled to −78 °C in an acetone−dry ice bath before the gas above the solution was transferred into a gas sample IR cell for analysis. Detection of the Q band at 3017 cm⁻¹, a strong absorption peak at 1306 cm⁻¹, and accompanying rotational fine structures confirmed the presence of CH_4. Comparison of the GC retention time of 1.665 min with the standard sample of CH_4 (t_R = 1.656 min) corroborated the presence of CH_4. Neither

vibrational absorption bands centered at 1450 and 730 cm^{-1} nor a GC retention time of 1.880 min due to ethane were detected. The gas was also analyzed by EI-MS, which showed methane but no ethane.

Thermolysis of 1b with TEMPO. Cluster **1b** (3.3 mg, 0.0030 mmol) and TEMPO (0.2 mg, 0.0013 mmol) were placed in an NMR tube fitted with a Teflon valve, with d_{20}-nonane (0.5 mL). The solution was degassed by three freeze−pump−thaw cycles and then heated at 125 °C for 10 h, whereupon the color of the solution turned from yellow to red. No TEMPO-CH$_3$ was detected in the ^{1}H NMR spectrum.

Thermolysis of 1b with 7. Clusters **1b** (190 mg, 0.172 mmol) and **7** (25 mg, 0.0276 mmol) were dissolved in n-octane (100 mL) and the solution was deoxygenated and then brought to reflux for 2 h, during which time the color of the solution turned from yellow to light orange. Removal of the solvent in vacuo and separation by TLC afforded unreacted **7** (28.4 mg), **2b** (27.2 mg, 15.1%), and unreacted **1b** (156.4 mg).

Thermolysis of 1c in Refluxing n-Octane. Cluster **1c** (193.0 mg, 0.165 mmol) was thermolyzed and worked up in a manner similar to that above to yield four bands on the TLC. In order of elution they are **7** (23.5 mg, 15.7%), Os$_3$(CO)$_9$(μ-H)(μ_3,η^2-C$_6$H$_4$)-(μ-SbPhMe) (**2c/2c′**; 77.5 mg, 42.2%), **2a** (15.7 mg, 8.1%), and unreacted **1c** (65.5 mg). Clusters **2c/2c′** and **2a** were separated by repeated TLC until the ^{1}H NMR showed that both bands were free from each other. Cluster **2a** probably arose from a small quantity of **1a** present in the sample of **1c**; these could not be separated by TLC. This is supported by the detection of SbPh$_3$ in the EI-MS of the SbMePh$_2$ solution used to prepare **1c**. The structure of the known cluster **2a** was established by a single-crystal X-ray crystallographic study as a solvate of that reported (Supporting Information).[23]

Data for **2c/2c′** are as follows. IR: ν(CO) 2090 (w), 2070 (vs), 2042 (vs), 2016 (m), 2009 (m), 2003 (m), 1988 (w), 1977 (w), 1971 (w) cm^{-1}. ^{1}H NMR for **2c** (CD$_2$Cl$_2$): δ 9.17 (d, 1H, $^3J_{HH}$ = 8.25 Hz, C$_6$H$_4$), 6.74 (dd, 1H, C$_6$H$_4$), 7.05 (dd, 1H, C$_6$H$_4$), 8.64 (d, 1H, C$_6$H$_4$), 7.22 − 7.19 (m, 3H, Ph), 6.93−6.90 (m, 2H, Ph), 1.83 (s, 3H, Me), −17.45 (s, 1H, OsHOs). ^{1}H NMR for **2c′** (CD$_2$Cl$_2$, 218 K): δ 9.17 (d, 1H, $^3J_{HH}$ = 8.25 Hz, C$_6$H$_4$), 6.74 (dd, 1H, C$_6$H$_4$), 7.05 (dd, 1H, C$_6$H$_4$), 8.64 (d, 1H, C$_6$H$_4$), 7.35−7.42 (m, 5H, Ph), 1.33 (s, 3H, Me), −17.38 (s, 1H, OsHOs). The ratio of **2c** to **2c′** was determined from ^{1}H NMR to be 1:1. Anal. Calcd for C$_{17}$H$_{11}$O$_9$Os$_3$Sb: C, 23.72; H, 1.18. Found: C, 23.86; H, 1.05.

Thermolysis of 1d in Refluxing n-Octane. A similar thermolysis and workup with **1d** (150.0 mg, 0.134 mmol) yielded, after TLC separation, **7** (8.5 mg, 7.0%), Os$_3$(μ-SbMe$_2$)(μ-H)(μ_3,η^2-C$_6$H$_3$-4-Me)(CO)$_9$ (**2d**; 71.5 mg, 50.1%), and unreacted **1d** (42.9 mg).

Data for **2d** are as follows. IR: ν(CO) 2089 (w), 2068 (vs), 2040 (vs), 2009 (vs), 2003 (m, sh), 1988 (w), 1976 (w), 1968 (w) cm^{-1}. ^{1}H NMR: δ 9.03 (d, $^3J_{HH}$ = 8.25 Hz, C$_6$H$_3$, major), 8.87 (s, $^3J_{HH}$ = 8.25 Hz, C$_6$H$_3$, minor), 8.84 (s, C$_6$H$_3$, major), 8.58 (d, C$_6$H$_3$, minor), 6.84 (d, C$_6$H$_3$, minor), 6.62 (d, C$_6$H$_3$, major), 2.34 (s, C$_6$H$_3$*Me*, minor), 2.28 (s, C$_6$H$_3$*Me*, major), 1.57 (s, 3H, SbMe$_2$), 1.11 (s, 3H, SbMe$_2$), −17.58 (s, 1H, OsHOs). Anal. Calcd for C$_{18}$H$_{13}$O$_9$Os$_3$Sb·$^1/_4$C$_6$H$_{14}$: C, 21.54; H: 1.53. Found: C, 21.34; H, 1.52. ^{1}H NMR confirmed the presence of hexane in the sample.

A similar thermolysis of **1e** also afforded **2d**, identified by the low-temperature ^{1}H NMR spectrum. Yield: 81.8 mg, 43.0%.

Thermolysis of 1f in Refluxing n-Octane. A similar thermolysis and workup with **1f** (200 mg, 0.175 mmol) afforded Os$_3$(μ-SbMe$_2$)-(μ_3,η^1:η^2:η^2-C$_6$H$_3$Me$_2$)(CO)$_9$ (**6**), which eluted together with unreacted **1f**. Fractional crystallization afforded **6** as red crystals, but these were invariably contaminated with **1f**. Yield: ∼68.0 mg, 38.5%. IR: ν(CO) 2069 (w), 2044 (vs), 2022 (s), 1995 (m), 1985 (w), 1976 (w), 1968 (m), 1956 (w) cm^{-1}. ^{1}H NMR (CD$_2$Cl$_2$): δ 6.46 (1H, s, C$_6$*H*$_3$Me$_2$), 6.24 (1H, s, C$_6$*H*$_3$Me$_2$), 4.30 (1H, s,

C$_6$*H*$_3$Me$_2$), 2.89 (3H, s, C$_6$H$_3$*Me*$_2$), 2.11 (3H, s, C$_6$H$_3$*Me*$_2$), 1.80 (3H, s, SbMe$_2$), 1.43 (3H, s, SbMe$_2$). FAB-MS: m/z 1078.8 (calcd for [M$^+$] 1078.1).

Thermolysis of 1g in Refluxing n-Octane. A similar thermolysis and workup with **1g** (200 mg, 0.191 mmol) afforded **7** (2.9 mg, 1.7%), "Os$_3$SbMe$_3$(CO)$_{10}$" (**8**; 1.8 mg), unreacted **1g** (187.7 mg), and an unidentified band (0.3 mg; IR ν(CO) 2062 (m), 2055 (m), 2021 (vs), 2003 (s), 1991 (m), 1957 (m) cm^{-1}).

Data for **8** are as follows. IR: ν(CO) 2101 (vw), 2075 (m), 2064 (s), 2059 (vw), 2053 (vw), 2039 (s), 2019 (s), 2006 (w), 1996 (m), 1977 (m) cm^{-1}. ESI-MS (negative mode): 1049 (calcd for [M + OMe]$^-$ 1048.8).

Thermolyses of 2b. A sample of **2b** (1.5 mg, 0.0014 mmol) was placed in an NMR tube with d_8-toluene (0.5 mL), degassed by three freeze−pump−thaw cycles, and then heated at 90 °C for 4 h. The color of the solution remained yellow. The ^{1}H NMR spectrum in the hydride region revealed a single peak at −17.58 ppm (CDCl$_3$, 300 K). TLC analysis revealed the presence of unreacted **2b** only.

A similar thermolysis of **2b** (8.4 mg, 0.0080 mmol) with decane (10 mL) in a Carius tube at 150 °C was monitored by IR spectroscopy at 15 min intervals for 1 h. Cluster **5** was detected as the methoxide adduct in the ESI-MS spectrum. At the end of the thermolysis, the color of the solution was brown. TLC separation with hexane/dichloromethane (90:10, v/v) yielded **5** as the only identifiable product (2.3 mg, 29%).

A similar thermolysis of **2b** (10.1 mg, 0.0094 mmol) in refluxing n-octane (10 mL) under a constant nitrogen purge was monitored by IR spectroscopy at 30 min intervals for 4 h. At the end of the thermolysis, the color of the solution remained yellow. The IR spectrum and TLC analysis revealed **2b** as the only product present.

Thermolyses of 3. A sample of **3** (17.8 mg, 0.0165 mmol) in octane (10 mL) was refluxed in a 25 mL round-bottom flask. The solution turned from yellow to dark orange in 60 min. After removal of the octane in vacuo, the dark orange residue was dissolved in a minimal amount of dichloromethane and subjected to TLC separation with hexane as eluant. The first band (yield 0.9 mg, 5.2%) was identified as **2b**; four other unidentified bands were also obtained, together with a great deal of material remaining at the bottom.

Thermolysis of 1g and 2c/2c′. Clusters **1g** (2.1 mg, 0.0020 mmol) and **2c/2c′** (2.0 mg, 0.0018 mmol) were placed in a Carius tube with n-octane (10 mL), degassed by three freeze−pump−thaw cycles, and then heated at 140 °C for 30 min, whereupon the color of the solution turned from yellow to red. The ESI-MS spectrum showed peaks at m/z 1918.4 and 1945.3 only, corresponding to M$^+$ and [M + OMe]$^+$ for **4**.

X-ray Crystallographic Studies. Crystals were grown from dichloromethane/hexane solutions and mounted on quartz fibers. X-ray data were collected on a Bruker AXS APEX system, using Mo Kα radiation, at 223 K with the SMART suite of programs.[24] Data were processed and corrected for Lorentz and polarization effects with SAINT[25] and for absorption effects with SADABS.[26] Structural solution and refinement were carried out with the SHELXTL suite of programs.[27] Crystal and refinement data are summarized in Tables 5 and 6.

The structures were solved by direct methods to locate the heavy atoms, followed by difference maps for the light, non-hydrogen atoms. There were two crystallographically independent molecules in the asymmetric units of **1d** and **3**. A dichloromethane solvent molecule was found in **2a** and a hexane molecule (half occupancy) in **6**. The locations of the hydrides were either located in a low angle difference map (**2a**, **2c**, **2d**, and **5**) or placed by potential

(23) Leong, W. K.; Chen, G. *Organometallics* **2001**, *20*, 2280.

(24) SMART, version 5.628; Bruker AXS Inc., Madison, WI, 2001.
(25) SAINT+, version 6.22a; Bruker AXS Inc., Madison, WI, 2001.
(26) Sheldrick, G. M. SADABS, 1996.
(27) SHELXTL, version 5.1; Bruker AXS Inc., Madison, WI, 1997.

Table 5. Crystal and Refinement Data for 1b,d and 2b−d

	1b	1d	2b	2c	2d
empirical formula	$C_{19}H_{11}O_{11}Os_3Sb$	$C_{20}H_{13}O_{11}Os_3Sb$	$C_{17}H_{11}O_9Os_3Sb$	$C_{22}H_{13}O_9Os_3Sb$	$C_{18}H_{13}O_9Os_3Sb$
formula wt	1107.63	1121.65	1051.61	1113.67	1065.63
temp, K	223(2)	223(2)	223(2)	298(2)	223(2)
cryst syst	monoclinic	monoclinic	monoclinic	monoclinic	monoclinic
space group	$C2/c$	$P2_1/c$	$P2_1/c$	$P2_1/n$	$C2/c$
a, Å	21.8809(9)	8.4121(5)	16.3554(14)	8.4185(2)	9.6232(5)
b, Å	8.3103(4)	35.499(2)	10.2881(9)	16.8901(5)	16.1907(8)
c, Å	27.3697(12)	17.5220(11)	13.2426(11)	18.1308(5)	29.7325(15)
β, deg	90.1010(10)	96.161(3)	96.605(2)	96.8350(10)	96.2140(10)
V, Å^3	4976.8(4)	5202.2(6)	2213.5(3)	2559.68(12)	4605.3(4)
Z	8	8	4	4	8
density (calcd), Mg/m^3	2.957	2.864	3.156	2.890	3.074
abs coeff, mm^{-1}	16.396	15.688	18.417	15.935	17.706
F(000)	3936	4000	1856	1984	3776
cryst size, mm^3	0.30 × 0.24 × 0.18	0.16 × 0.14 × 0.03	0.16 × 0.14 × 0.08	0.32 × 0.30 × 0.20	0.12 × 0.08 × 0.06
θ range for data collecn, deg	2.38−30.01	2.08−26.37	2.34−24.71	2.26−29.52	2.47−26.37
no. of rflns collected	38 510	39 232	23 020	19 891	30 314
no. of indep rflns	7257 (R(int) = 0.0497)	10640 (R(int) = 0.0684)	3771 (R(int) = 0.0374)	6436 (R(int) = 0.0374)	4712 (R(int) = 0.0381)
max, min transmissn	0.1563, 0.0838	0.6504, 0.1880	0.3205, 0.1566	0.1428, 0.0801	0.4164, 0.2251
no. of data/restraints/params	7257/0/309	10 640/0/637	3771/0/183	6436/0/321	4712/0/286
goodness of fit on F^2	1.173	1.137	1.227	1.029	1.358
final R indices ($I > 2\sigma(I)$)	R1 = 0.0326, wR2 = 0.0574	R1 = 0.0585, wR2 = 0.1047	R1 = 0.0498, wR2 = 0.1155	R1 = 0.0333, wR2 = 0.0709	R1 = 0.0533, wR2 = 0.1003
R indices (all data)	R1 = 0.0404, wR2 = 0.0591	R1 = 0.0840, wR2 = 0.1123	R1 = 0.0552, wR2 = 0.1176	R1 = 0.0469, wR2 = 0.0754	R1 = 0.0569, wR2 = 0.1014
largest diff peak, hole, e Å^{-3}	1.253, −1.144	2.171, −1.280	3.703, −1.409	1.639, −1.520	2.257, −1.478

Table 6. Crystal and Refinement Data for 3−6

	3	4	5	6
empirical formula	$C_{18}H_{11}O_{10}Os_3Sb$	$C_{27}H_7O_{20}Os_6Sb$	$C_{31}H_{18}O_{16}Os_6Sb_2$	$C_{22}H_{22}O_9Os_3Sb$
formula wt	1079.62	1914.28	2031.15	1122.75
temp, K	223(2)	298(2)	223(2)	223(2)
cryst syst	monoclinic	monoclinic	monoclinic	monoclinic
space group	Pn	$P2_1/n$	$P2_1/c$	$P2_1/n$
a, Å	9.2722(4)	9.6092(3)	15.7364(10)	9.8025(6)
b, Å	15.0937(7)	27.4384(8)	13.2779(8)	18.0300(10)
c, Å	17.2511(8)	14.3351(4)	19.5943(12)	15.8402(9)
β, deg	90.7010(10)	92.5710(10)	91.037(2)	103.4880(10)
V, Å^3	2414.14(19)	3775.80(19)	4093.5(4)	2722.4(3)
Z	4	4	4	4
density (calcd), Mg/m^3	2.970	3.367	3.296	2.739
abs coeff, mm^{-1}	16.894	20.889	19.908	14.984
F(000)	1912	3344	3560	2020
cryst size, mm^3	0.40 × 0.34 × 0.10	0.20 × 0.08 × 0.02	0.16 × 0.09 × 0.04	0.18 × 0.12 × 0.10
θ range for data collecn, deg	2.36−29.93	2.06−28.28	2.01−24.71	2.24−29.55
no. of rflns collected	19 935	49 800	40 328	38 009
no. of indep rflns	6429 (R(int) = 0.0512)	9046 (R(int) = 0.0469)	6982 (R(int) = 0.0304)	7137 (R(int) = 0.0275)
max, min transmissn	0.2829, 0.0565	0.6801, 0.1027	0.5031, 0.1429	0.3157, 0.1734
no. of data/restraints/params	6429/2/581	9046/0/488	6982/0/502	7137/66/369
goodness of fit on F^2	1.032	1.096	1.193	1.059
final R indices ($I > 2\sigma(I)$)	R1 = 0.0325, wR2 = 0.0708	R1 = 0.0444, wR2 = 0.0781	R1 = 0.0342, wR2 = 0.0685	R1 = 0.0303, wR2 = 0.0644
R indices (all data)	R1 = 0.0358, wR2 = 0.0721	R1 = 0.0608, wR2 = 0.0832	R1 = 0.0382, wR2 = 0.0700	R1 = 0.0362, wR2 = 0.0667
largest diff peak, hole, e Å^{-3}	3.017, −1.757	1.917, −0.973	1.490, −1.065	1.699, −0.924

energy calculations (**2b** and **3**) with the program XHYDEX.[28] They were refined fully (**2c**), refined on position only (**2a**, **2d**, and **5**), or refined riding on one of the osmium atoms they are attached to (**2b** and **3**) with fixed isotropic thermal parameters. Organic hydrogen atoms were placed in calculated positions and refined with a riding model. All non-hydrogen atoms were generally given anisotropic displacement parameters in the final model, except for the carbon atoms in **2a** and **2b**, where there appeared to be problems due to extreme absorption differences which could not be adequately corrected for. The structure of **3** was refined as a racemic twin.

Supporting Information Available: Crystallographic data in CIF format and text and figures giving experimental details on the syntheses and characterization of the stibines and clusters **1**. This material is available free of charge via the Internet at http://pubs.acs.org.

(28) Orpen, A. G. XHYDEX; School of Chemistry, University of Bristol, Bristol, U.K., 1997.

OM0508132